Peimine induces apoptosis of glioblastoma cells through regulation of the PI3K/AKT signaling pathway

JIAMING LEI[1,2*], JIANBAO YANG[3*], SHIJIAO CHENG[1,2], FEIFEI LU[1,2], ZIHAN WU[4], ZIYI WANG[5], ZIQI WANG[5], CHENYU SUN[5] and LI LIN[2]

[1]School of Pharmacy, Xianning Medical College, Hubei University of Science and Technology, Xianning, Hubei 437100, P.R. China; [2]Key Laboratory of Environmental Related Diseases and One Health, School of Basic Medical Sciences, Xianning Medical College, Hubei University of Science and Technology, Xianning, Hubei 437100, P.R. China; [3]School of Public Health, Xianning Medical College, Hubei University of Science and Technology, Xianning, Hubei 437100, P.R. China; [4]Department of Ultrasound, Xianning Traditional Chinese Medicine Hospital, Xianning, Hubei 437100, P.R. China; [5]Department of Medicine, Hubei University of Science and Technology, Xianning, Hubei 437100, P.R. China

Received May 13, 2024; Accepted August 22, 2024

DOI: 10.3892/etm.2024.12737

Abstract. Glioblastoma (GBM) is one of the most malignant forms of intracranial tumors, with high mortality rates and invariably poor prognosis, due to the limited clinical treatment strategies available. As a natural compound, peimine's favorable pharmacological activities have been widely revealed. However, potential inhibitory effects of peimine on GBM have not been explored. In the present study, both *in vitro* and *in vivo* experiments were performed to elucidate the effects of peimine on GBM and to further delineate the underlying molecular mechanism of action. Different doses (0, 25 and 50 μM) of peimine were added to U87 cells, before MTT, colony formation, wound healing, Transwell migration and invasion, reactive oxygen species and mitochondrial transmembrane potential assays were used to measure proliferation, migration, invasion and apoptosis. Furthermore, western blotting was used to examine the possible effects of peimine on the expression of proteins associated with apoptosis and the PI3K/AKT signaling pathway. Subsequently, a GBM mouse xenograft model was used to assess the effects of peimine *in vivo*. The findings showed that peimine inhibited GBM proliferation, migration and invasion in a dose-dependent manner, whilst also inducing apoptosis. Peimine also reduced tumor growth *in vivo*. Mechanistically, peimine downregulated the expression of Bcl-2 and Caspase 3, whilst upregulating the protein expression levels of p53, Bax and Cleaved-Caspase 3 in a dose-dependent manner. In addition, PI3K and AKT phosphorylation levels were found to be decreased by peimine in a dose-dependent manner. In conclusion, these findings suggest that peimine may limit GBM growth by regulating the PI3K/AKT signaling pathway both *in vitro* and *in vivo*. These findings may have promising clinical implications.

Correspondence to: Professor Li Lin, Key Laboratory of Environmental Related Diseases and One Health, School of Basic Medical Sciences, Xianning Medical College, Hubei University of Science and Technology, 88 Xianning Avenue, Xianning, Hubei 437100, P.R. China
E-mail: alison1012li@163.com

*Contributed equally

Abbreviations: BBB, blood-brain barrier; GBM, glioblastoma

Key words: glioblastoma, peimine, apoptosis, proliferation, PI3K/AKT

Introduction

Glioblastoma multiforme (GBM) is one of the most common and lethal primary brain malignancies in adults, causing a yearly average of 3.19 new cases per 100,000 individuals (1,2). Despite the availability of a variety of post-neurosurgical treatment options, including temozolomide, radiotherapy and certain targeted drugs, such as bevacizumab, panitumumab and entrectinib, the prognosis for patients with GBM remains poor. GBM is also the most lethal primary brain malignancy, causing a 2-year survival rate of 26-33%, a 4-5% survival rate at 5 years, and a median survival time of just 15 months (3,4). The blood-brain barrier (BBB) represents a primary obstacle, significantly limiting the effectiveness of anticancer drugs in patients with GBM (5,6). Therefore, it is imperative to investigate and identify novel potential therapeutic options that can cross the BBB for managing GBM. Natural small-molecule compounds offer several advantages, including the wide range of sources from which they can be obtained, their ability to easily penetrate the BBB and their capacity to inhibit tumor growth through multiple mechanisms (7).

In recent years, identifying novel natural small-molecule compounds for the targeted therapy of GBM is becoming a field of intense research (8). Peimine is the primary compound extracted from the Himalayan frillitary lily *Bulbus Fritillariae* (BF), which is an established Traditional Chinese Medicine. BF has been known for >2,000 years for its antitussive and

antiasthma properties, in addition to boasting high therapeutic efficacy, reported low toxicity and minimal side effects, in diseases such as osteoarthritis (9). Peimine is a coumarin derivative, with various pharmacological mechanisms of action, such as anti-inflammatory, pain inhibitory and anti-asthma actions (10-12). It has been previously reported that peimine exhibits anticancer properties across various malignancies, such as breast, gastric and prostate cancer (13-15). However, it remains unclear whether it can exert an inhibitory effect on GBM.

Therefore, the present study investigated the potential effects of peimine on GBM both *in vitro* and *in vivo*, whilst also determining its possible underlying mechanism of action.

Materials and methods

Materials and reagents. Peimine was purchased from Shanghai Yuanye Bio-Technology Co., Ltd. Unless otherwise stated, all compounds were dissolved in DMSO. Procell Life Science & Technology Co., Ltd. provided the human GBM cell lines U87 (cat. no. CL-0238) and U251 (cat. no. CL-0237), in addition the normal human brain glial cell line HEB (cat. no. CL0130). The U87 cell line used was the U87-MG ATCC (CVCL 0022) cell line (HTB-14) and was authenticated using STR analysis. U87, U251, HEB and GL261 cells were cultured in DMEM (Gibco; Thermo Fisher Scientific, Inc.) supplemented with 10% FBS and 1% penicillin-streptomycin (Gibco; Thermo Fisher Scientific, Inc.), with high glucose and high glutamine levels. All cells were cultured at 37˚C in a humidified incubator supplied with 95% air and 5% CO_2.

Cell viability assay. In total, $8x10^3$ U87, U251 and HEB cells were plated in 96-well plates and incubated for 24 h at 37˚C. Following incubation, AKT activator SC79 (10 μM), AKT inhibitor MK2206 (10 μM) or peimine (0 or 25 μM) were added to the wells. The treatment time was 1, 24 and 24 h at 37˚C, respectively. Subsequently, 10 μl MTT solution was added to each well and incubated for 4 h at 37˚C. To dissolve the formazan crystals, 100 μl DMSO was added. Next, the plates were vortexed at room temperature for 10 min. The Bio-Tek ELX800 Multi-Mode Reader (BioTek Instruments, Inc.) was used to measure absorbance at 490 nm.

Colony formation assay. Trypsin was used to lift U87 cells during the logarithmic growth phase. The cell suspension was then resuspended using 1 ml DMEM and counted. In a 6-well plate, 1,000 cells were then plated in each well for each experimental group. The cells were cultured for 14 days at 37˚C or until the majority of the single clones had ≥50 cells. Every 3 days, the medium was changed and the condition of the cells was routinely checked. After the 14-day growth period, cells were once again washed with PBS and imaged under a microscope. After fixing each well for 30 min with 1 ml 4% paraformaldehyde at 26˚C, the cells were washed again with PBS. The cells were then stained for 20 min with 1 ml at 26˚C crystal violet staining solution. Subsequently, the cells were washed several times with PBS at 26˚C, dried and imaged using a digital camera (16).

Wound healing assay. In 6-well plates, U87 cells in the logarithmic growth phase were trypsinized, before $3x10^5$ were resuspended and seeded into each well. Cells were cultured until the confluence reached ~95% at 37˚C, then a 200-μl pipette tip was used to create a wound in the monolayer of cells. The culture media was removed from the wells, the monolayer of cells was washed twice and then 0, 25 or 50 μM of 2 ml peimine solution was added. Images of wound closure were captured at 0 and 24 h. After 24 h at 37˚C, the culture media was aspirated, the wells were washed twice with PBS and then imaged using an X71 fluorescence microscope (Olympus Corporation).

Cell migration and invasion assays. Using the Transwell inserts (0.4-μm pore size; Corning, Inc.), the effects of peimine on the invasion and migration of U87 cells were evaluated. For migration assays, a total of $5x10^3$ cells per well in 200 μl serum-free media was added into the upper chamber of a Transwell insert in a 24-well plate. A total of 600 μl DMEM containing the 0, 25 or 50 μM peimine was added to the lower chamber. For invasion assays, Matrigel (Corning, Inc.) diluted 1:8 (60 μl) was first added to the upper chamber of the insert and once it had solidified on a cell culture incubator for 1 h at 37˚C, cells were added to the upper chamber and media was added to the lower chamber in the same manner as the migration assay. Cells were incubated for 24 h at 37˚C, before cells that had passed through the Transwell membrane were fixed for 20 min using 4% paraformaldehyde at 26˚C and then stained for 20 min using 1% crystal violet at 26˚C. Images were taken using an X71 fluorescent microscope (Olympus Corporation) and data was analyzed with Image J software (version 1.53e; National Institutes of Health).

Reactive oxygen species (ROS) analysis. The production of ROS is inevitable for aerobic organisms, which occurs at a controllable rate in healthy cells. Under oxidative stress conditions, ROS production increases sharply, causing changes in membrane lipids, proteins and nucleic acids. The oxidative damage of these biomolecules is associated with cancer. Dichloro fluorescein (DCF), the fluorescent oxidized product of 2',7'-dichlorofluorescin diacetate (DCFDA; MilliporeSigma), was used to measure intracellular ROS levels. First, $1.5x10^5$ U87 cells were plated into 6-well plates and pre-treated for 6 h at 37˚C with either DMEM or 3 mM N-acetyl-L-cysteine (MilliporeSigma). Peimine (0, 25 or 50 μM) was then added to the media and cells were treated for a further 8 h at 37˚C, after which the media was replaced with fresh complete media containing 2 μg DCFDA for 6 min at 37˚C in the dark. Using an X71 fluorescent microscope, the proportion of apoptotic cells was determined.

Mitochondrial transmembrane potential assay. Membrane permeability JC-1 staining is widely used in apoptosis studies to monitor mitochondrial health. JC-1 staining reagent showed potential-dependent accumulation in mitochondria. At low concentration, it existed as monomer and produced green fluorescence at ~529 nm. Carbonyl cyanide 3-chlorophenylhydrazone (CCCP; Biosharp Life Sciences) was selected as the positive control. U87 cells ($2.5x10^4$) were treated with 0, 25 or 50 μM peimine for 24 h at 37˚C. Next, cells were collected, centrifuged for 5 min at 26˚C (1,400 x g) and resuspended in PBS. CCCP (10 mM) was added to the cell culture medium at a ratio of 1:1,000, diluted to 10 μM, and the cells were treated

with 200 μl for 20 min at 37˚C. The cells were then centrifuged again, resuspended in binding buffer and incubated for 30 min at 37˚C in the dark with 200 μl the JC-1 probe (Biosharp Life Sciences). Cells were then resuspended in 500 μl pre-cooled PBS and rinsed twice. An X71 fluorescent microscope was used to calculate the proportion of apoptotic cells.

Annexin V-FITC/PI staining assay. U87 cells ($2.5x10^4$) in 24-well plates (Costar; Corning, Inc.) were treated with 0, 25 or 50 μM of peimine for 24 h at 37˚C. Cells were then harvested, centrifuged for 5 min at 26˚C (1,400 x g) and resuspended in PBS. After re-suspending in binding buffer, $1.5x10^5$ U87 cells were stained using the Annexin V-FITC/PI kit (cat. no. BL1884A; Biosharp Life Sciences) for 20 min at 37˚C. The percentage of apoptotic cells was then determined using an X71 fluorescence microscope. Staining quality [apoptotic cells were double positive (Annexin V^+/PI^+) by FITC and PI binding staining] was analyzed by Image J software (version 1.53e; National Institutes of Health).

GBM subcutaneous xenograft model. Hubei University of Science and Technology Animal Ethics Committee approved the animal experiments (approval no. 2022-11-027) and all procedures adhered to national and international standards for the care and use of animals in research. GL261 GBM cells (cat. no. CTCC-400-0404; Zhejiang Meisen Cell Technology Co., Ltd.) were used to establish the mouse model. In total, 5-week-old male C57BL/6 mice (n=3/group; total, n=9) weighing 20-24 g were selected for the study. GL261 cells were subcutaneously injected into the right back of each mouse with $5x10^6$ cells in 100 μl sterile PBS. After the tumor reached a mean volume of ~100 mm^3, mice were divided into the following three groups at random: Control; low-dose (20 mg/kg); and high-dose (40 mg/kg) (17). Body weights were recorded daily and tumor volumes were measured every 2 days using the following formula: Volume=a x b^2 x 0.52, where a is the length and b is the width in mm. Mice in the low-dose and high-dose groups were treated intragastrically every 2 days with 20 or 40 mg/kg peimine, respectively. Control mice received saline instead of peimine. The mice were sacrificed under anesthesia (intraperitoneal injection of sodium pentobarbital 100 mg/kg) after 14 days. Death was confirmed by a lack of response to a toe pinch, lack of breathing and lack of heartbeat. Samples from the tumors and livers in the animals were then collected for additional examination.

H&E staining. Liver tissues from mice were fixed using 4% paraformaldehyde for 24 h at 26˚C, dehydrated and embedded in paraffin. The samples were fixed in 10% formalin for 12 h at 4˚C, and then embedded in paraffin for subsequent sectioning. The 4-μm specimens were first placed in distilled water and then in an aqueous solution of hematoxylin for staining for ~10 min at room temperature. After which, the slices were placed into ammonia and acid water for several seconds, and then rinsed in running water for 1 h. The sections were placed in distilled water for several seconds, after which they were dehydrated in alcohol at concentrations of 90 and 70% for 10 min each. Subsequently, the sections were stained with eosin staining solution for 2-3 min at room temperature. After staining, the samples were dehydrated with 100% alcohol and placed in xylene. The sections were sealed and placed in an incubator for drying. H&E staining (cat. no. BL700A; Biosharp Life Sciences) was performed on the liver tissues for toxicological analysis using light microscropy.

Western blot analysis. Treated U87 cells were first collected, washed three times with ice-cold PBS and then lysed using RIPA lysis buffer (cat. no. P0013B; Beyotime Institute of Biotechnology) supplemented with protease and phosphatase inhibitors (Beyotime Institute of Biotechnology) for 30 min. The resultant lysate was centrifuged and the supernatant was collected (4˚C, 15 min and 14,000 x g). A BCA assay kit (Beyotime Institute of Biotechnology) was used to measure the protein content according to the manufacturer's protocol. Loading buffer was added to the protein samples and then boiled at 100˚C for 10 min. Next, the protein samples (40 μg/lane) were loaded on 8-10% SDS gels, resolved using SDS-PAGE, transferred onto PVDF membranes and the membranes were blocked (5% skimmed milk for 1 h at 26˚C). Following blocking, the membranes were incubated with the indicated primary antibodies overnight at 4˚C. The following day, the membranes were washed, and incubated with the HRP-conjugated secondary antibodies at 26˚C. Signals were visualized using ECL plus reagent (Beyotime Institute of Biotechnology). GAPDH was used as the loading control. The following antibodies were used: p53 (1:1,000; cat. no. R380701), Bax (1:1,000; cat. no. R22708), Bcl-2 (1:1,000; cat. no. R23309), Caspase 3 (1:1,000; cat. no. R23315), Cleaved-Caspase 3 (1:1,000; cat. no. 341034) (all Chengdu Zen-Bioscience Co., Ltd.), phosphorylated (p)-PI3K (1:1,000; cat. no. AP1463), PI3K (1:1,000; cat. no. A19742), p-AKT (1:1,000; cat. no. AP1259), AKT (1:1,000; cat. no. A17909), GAPDH (1:1,000; cat. no. 390035) and HRP Goat Anti-Mouse IgG (1:1,000, cat. no. AS003) (all ABclonal Biotech Co., Ltd.). The blot densities were quantified using ImageJ software (version 1.53e; National Institutes of Health).

Statistical analysis. Experimental data were analyzed by Image J (version 1.53e) and SPSS 27.0 software (IBM Corp.). GraphPad prism 8.0 software (Dotmatics) was used for visualization. Data are presented as the mean ± SD. Data were analyzed using a one-way ANOVA followed by Tukey's post hoc test using SPSS 27.0 software (IBM Corp.). $P<0.05$ was considered to indicate a statistically significant difference.

Results

Peimine inhibits GBM cell proliferation. MTT assays were performed to assess the viability of HEB, U87 and U251 cells following treatment with various concentrations of peimine (0, 6.25, 12.5, 25, 50 or 100 μM; Fig. 1B-D). The results showed a dose-dependent reduction of GBM cell viability caused by peimine. Compared with the control group, with the increase of drug concentration, GBM cell viability was inhibited to an marked degree, but there were no obvious effects of peimine on HEB cells (Fig. 1B). In U87 and U251 cells, the IC_{50} values were found to be 21.3 and 92.8 μM, respectively after 48 h of treatment. By contrast, the IC_{50} value was 39.9 μM in U87 cells treated for 24 h. As the IC_{50} of U87 cells is much lower than that of U251 cells, for subsequent experiments, 25 and 50 μM

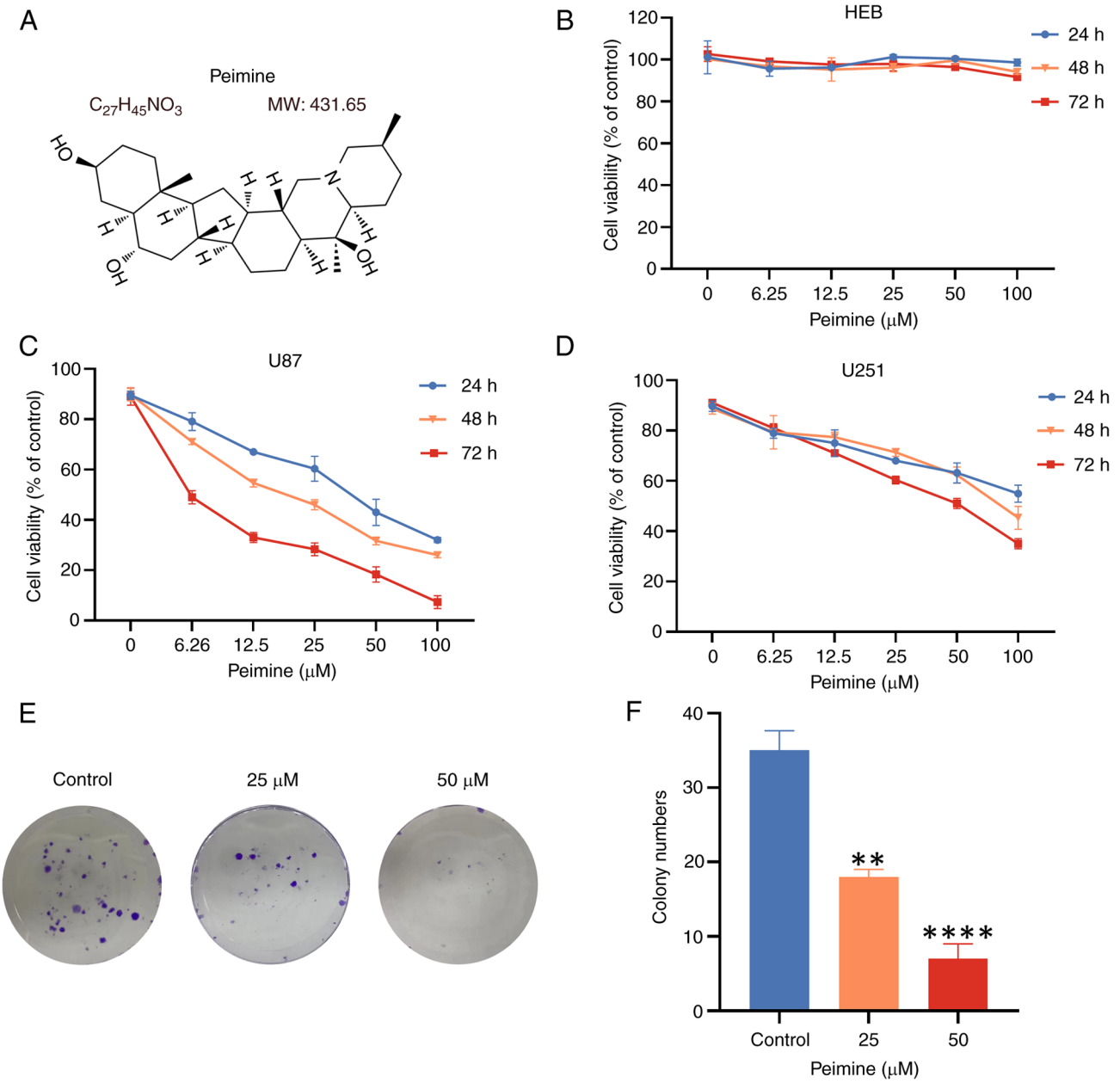

Figure 1. Effects of peimine on the cell viability and colony formation of glioblastoma cells. (A) The chemical structure of peimine. (B) HEB, (C) U87 and (D) U251 cells were treated with different doses of peimine (0, 6.25, 12.5, 25, 50 and 100 μM) for 24, 48, and 72 h. An MTT assay was used to determine the viability of the cells. (E) Colony formation assays were performed using U87 cells, (F) which were quantified. Data are presented as the mean ± SD from three repeats. Data were analyzed using a one-way ANOVA followed by a Tukey's post-hoc test. **P<0.01 and ****P<0.0001 vs. the control.

peimine was used for U87 cells based on the IC_{50} value, with a treatment duration of 24 h.

A colony formation assay was next used to assess the proliferation of U87 cells. Treatment of U87 cells with varying concentrations of peimine resulted in a dose-dependent decrease in colony formation. Notably, significant differences in colony formation ability were observed in cells treated with 25 and 50 μM peimine compared with that in cells treated with 0 μM peimine, demonstrating that peimine had an inhibitory effect on the growth of GBM cell colonies (Fig. 1E and F). These findings suggest the inhibitory effects of peimine on GBM cell proliferation, with minimal toxicity and side effects observed in HEB cells. This suggests that peimine exhibits selectivity for cancerous cells whilst maintaining a safe profile on normal cells, highlighting it as a promising candidate for further drug development.

Peimine inhibits GBM cell migration and invasion. Results from wound healing assays showed significant inhibition of U87 cell migration following 24 h of treatment with 25 and 50 μM peimine (Fig. 2A and B), where peimine dose-dependently reduced migration compared with that in the control group.

Similarly, Transwell assay results showed significantly reduced U87 cell migration and invasion following the 24 h peimine treatment in a dose-dependent manner (Fig. 2C and D). These results were consistent with the results of the wound healing assays. Together, these results suggest the inhibitory effect of peimine on the invasion and migration of GBM cells.

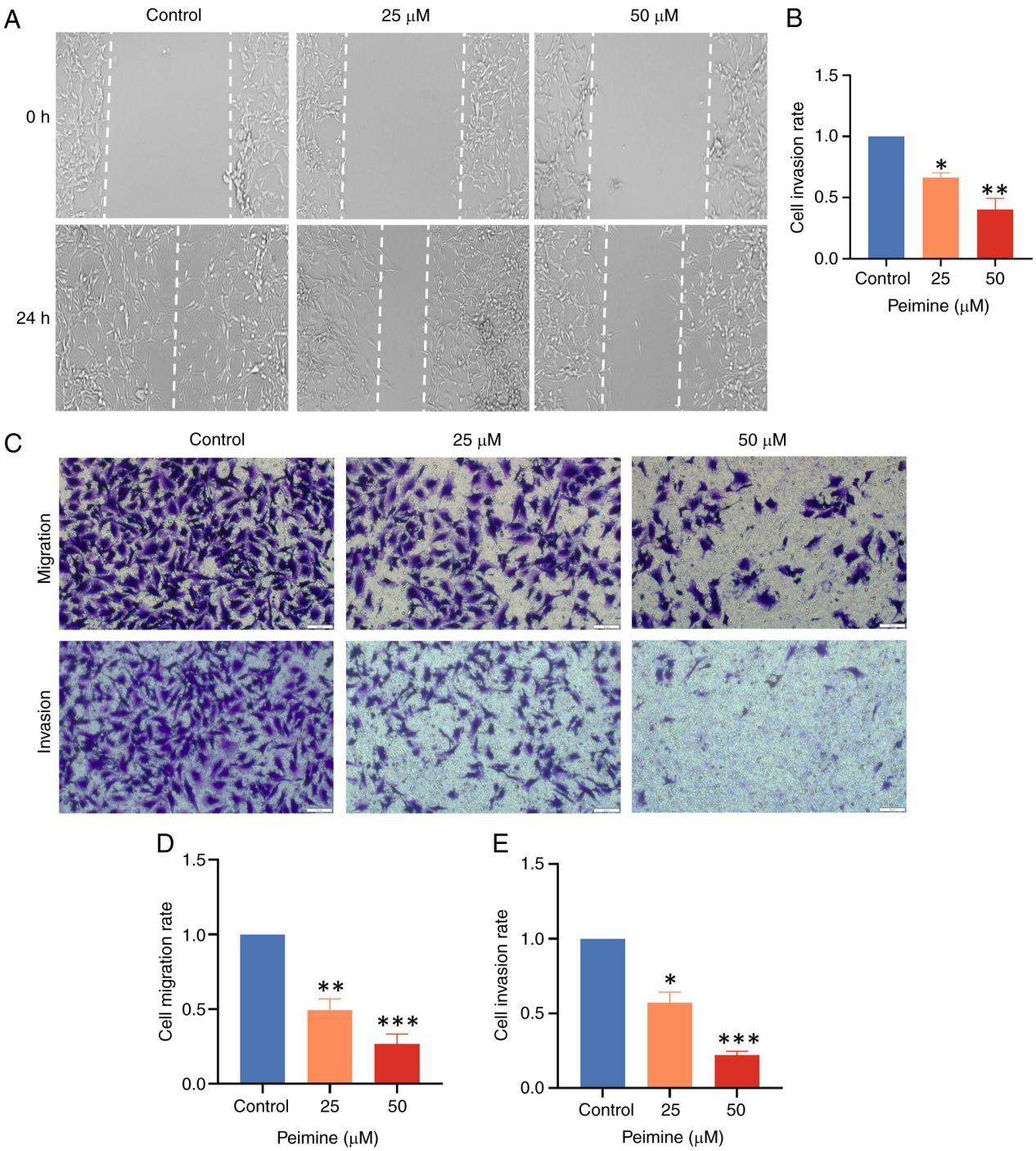

Figure 2. Peimine reduces migration and invasion of glioblastoma cells. (A) Wound healing assays were performed using U87 cells treated with peimine. Scale bar, 500 μm. (B) Quantification of wound healing assay. (C) Transwell assays were used to assess migration and invasion of U87 cells. Scale bar, 100 μm. Quantification of (D) migration and (E) invasion assays. Data are presented as the mean ± SD from three repeats. Data were analyzed using a one-way ANOVA followed by a Tukey's post-hoc test. *P<0.05, **P<0.01 and ***P<0.001 vs. the control.

Peimine exhibits anti-GBM activity in vivo. The possible inhibitory effects of Peimine on GBM *in vivo* was assessed using a mouse xenograft model. Tumor size, volume and weight were found to be markedly reduced in both the low (20 mg/kg) and high (40 mg/kg) dose groups compared with those in the control group (Fig. 3A-C). Peimine did not considerably alter the body weight of the mice, where at therapeutic doses, no negative side effects (such as marked weight loss) were noted (Fig. 3D-F). Additionally, as shown in Fig. 3E and F, there were no marked variations in the liver/body ratio, liver morphology or the sectional tissue morphology between the peimine-treated group and the control group. These results suggest that peimine can effectively reduce GBM growth *in vivo* whilst maintaining favorable safety profiles, highlighting its potential as a therapeutic option for the treatment of GBM.

Peimine induces GBM cell apoptosis. ROS serves a pivotal role in apoptosis, the excessive accumulation which in cells can induce apoptosis. As shown in Fig. 4A and B, based on DCFH-DA staining. Quantification of fluorescent images revealed a

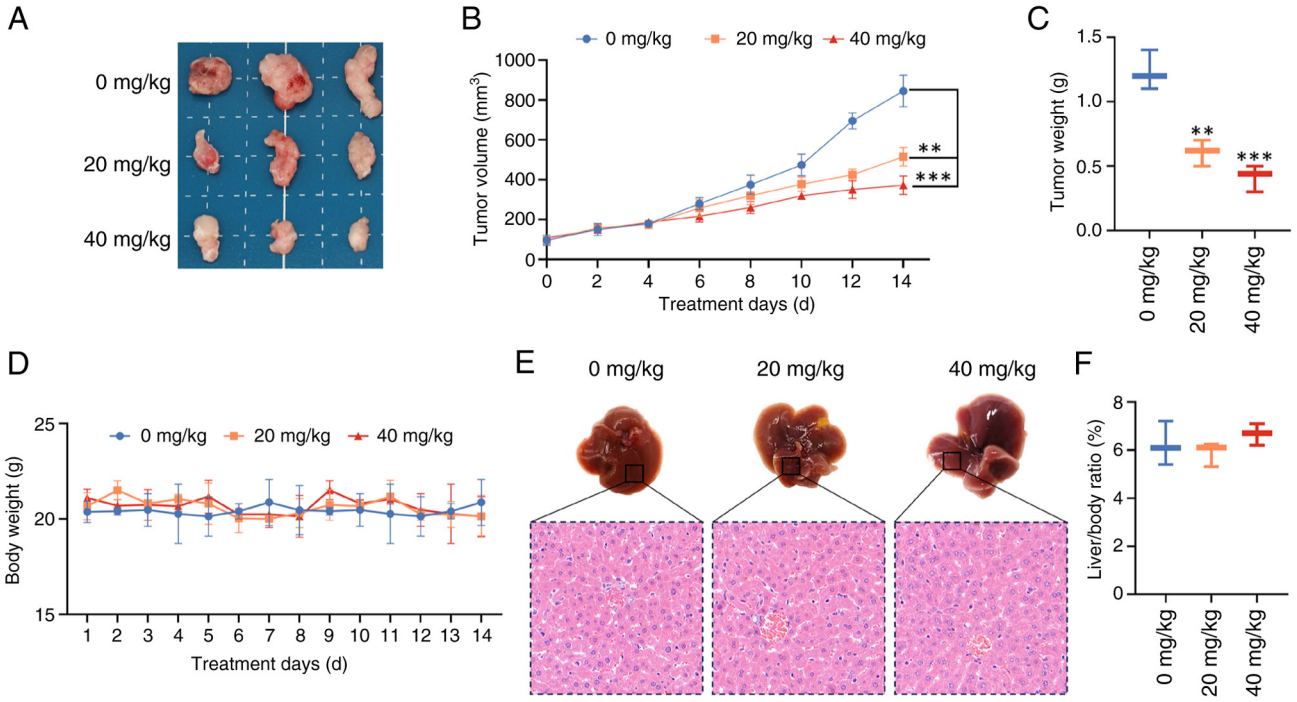

Figure 3. Peimine inhibits tumor development of glioblastoma in a xenograft mouse model. (A) At the experimental endpoint, tumors were excised and images were taken. (B) Tumor volume during the course of peimine therapy. (C) Tumor weights at the end of the experiment. (D) Body weight throughout the course of peimine therapy. (E) Images of the H&E-stained liver tissues from the xenograft mice treated with peimine. (F) Liver/body ratio of xenograft mice treated with peimine. Data are presented as the mean ± SD of three repeats. Data were analyzed using a one-way ANOVA followed by a Tukey's post hoc test. **P<0.01 and ***P<0.001 vs. 0 mg/kg.

significant increase in cellular ROS levels induced by peimine, indicative of increased oxidative damage. The mitochondrial membrane potential is typically altered during early apoptosis. The JC-1 probe was therefore next used to measure this change (Fig. 4C). CCCP, an apoptosis inducer serving as a mitochondrial oxidative phosphorylation uncoupling agent, was used as a positive control to denote a reduction of the mitochondrial membrane potential. As the peimine concentration increased, the quantity of JC-1 monomers (green) in GBM cells was increased, whilst that of JC-1 aggregates (red) was decreased, suggesting the induction of early apoptosis. Furthermore, U87 cell apoptosis induction was assessed further using Annexin V-FITC/PI staining (Fig. 4D and E). These results collectively suggest that peimine can induce apoptosis in GBM cells.

Peimine induces PI3K/AKT-dependent apoptosis in GBM cells. Western blot analysis was used to assess the effect of peimine on the expression of proteins associated with apoptosis in U87 cells (Fig. 5A and B). Following 24 h treatment with 25 and 50 μM peimine, Bcl-2 expression was found to be downregulated in a dose-dependent manner, whereas p53 and Bax expression were found to be upregulated. Furthermore, with 25 and 50 μM peimine, there was an increase in Cleaved-Caspase 3 expression.

Furthermore, to elucidate the molecular mechanism underlying peimine-mediated repression of proliferation and metastasis, the PI3K/AKT signaling cascade was next investigated, also using western blot analysis. The results showed that after treating U87 cells with peimine for 24 h, the levels of PI3K and AKT phosphorylation were found to be significantly decreased, in a dose-dependent manner (Fig. 5C and D).

To determine whether peimine can mediate apoptosis through AKT signaling, AKT signaling was activated or inhibited in cells. Rescue experiments were first conducted using 10 μM SC79, an AKT agonist. The results showed that the proliferative effects induced by peimine (25 μM) over 24, 48 and 72 h were nullified following pretreatment with SC79 for 1 h (Fig. 5E); however, this nullification was not significant. To further explore the mechanism of peimine on AKT signaling *in vitro*, the relationship between peimine activity and AKT pathway was explored using 10 μM MK2206, an AKT inhibitor (Fig. 5F). The combination of peimine and AKT inhibitor MK2206 had a stronger effect on the proliferation of U87 cells than peimine alone. Together, these results highlight the role of the PI3K/AKT signaling cascade in mediating the anti-tumor activities in GBM cells of peimine.

Discussion

GBM is an invasive primary malignant tumor that is difficult to treat, prone to relapse and exhibits a high mortality rate (18,19). Natural small-molecule compounds derived from plants used in Chinese herbal medicines are increasingly becoming an important source for the treatment of malignancies (20). The constituent components of Chinese herbal medicines, such as quercetin, lycorine and isobavachalcone, are also increasingly being studied for the identification of novel compounds to manage GBM (21-23).

The limited toxicities and side effects compared with conventional treatments, such as radiotherapy and chemotherapy, with additional capabilities of limiting tumor proliferation and apoptosis, have fueled further

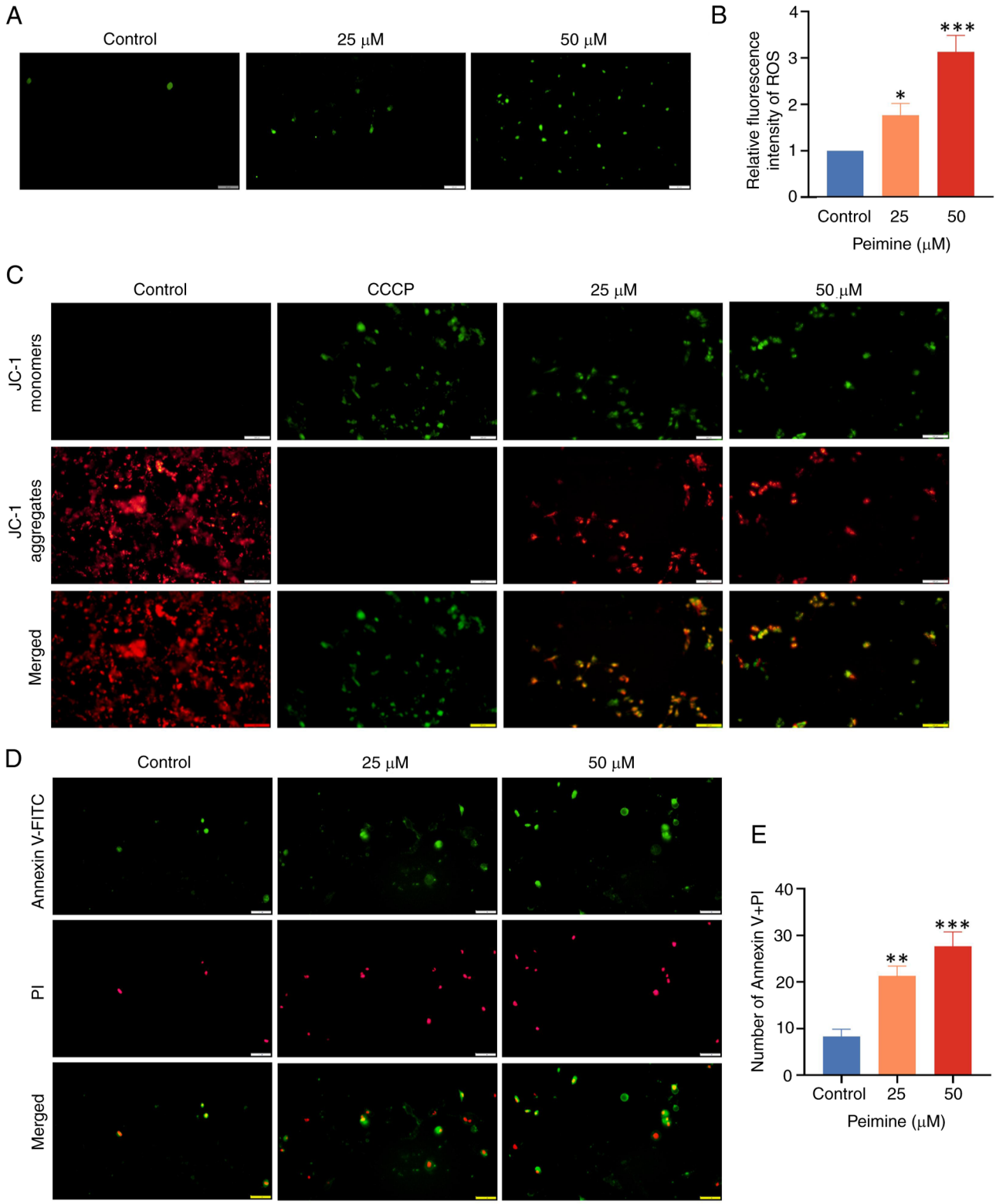

Figure 4. Peimine induces apoptosis in glioblastoma cells. (A) Following the treatment of U87 cells with varying doses of peimine, the ROS levels were measured. (B) Semiquantification of (A). (C) After peimine treatment for 24 h, the mitochondrial membrane potential of stained U87 cells was examined using a fluorescence microscope. (D) Apoptosis changes in stained U87 cells after peimine treatment for 24 h, performed by Annexin V-FITC/PI double staining. Scale bar, 100 μm. (E) Semi-quantification of (D). Data are presented as the mean ± SD of three repeats. Data were analyzed using a one-way ANOVA followed by a Tukey's post-hoc test. *P<0.05, **P<0.01 and ***P<0.001 vs. the control. ROS, reactive oxygen species.

research in this field (17). Despite its established efficacy in inducing cell death and inhibiting angiogenesis, their precise mechanisms of action remain to be fully elucidated. Researchers have found that eugenol enhances the chemotherapeutic potential of gemcitabine and induces anticarcinogenic and anti-inflammatory activity in human cervical cancer cells (24). The synergistic use of chemotherapeutic drugs with natural components can

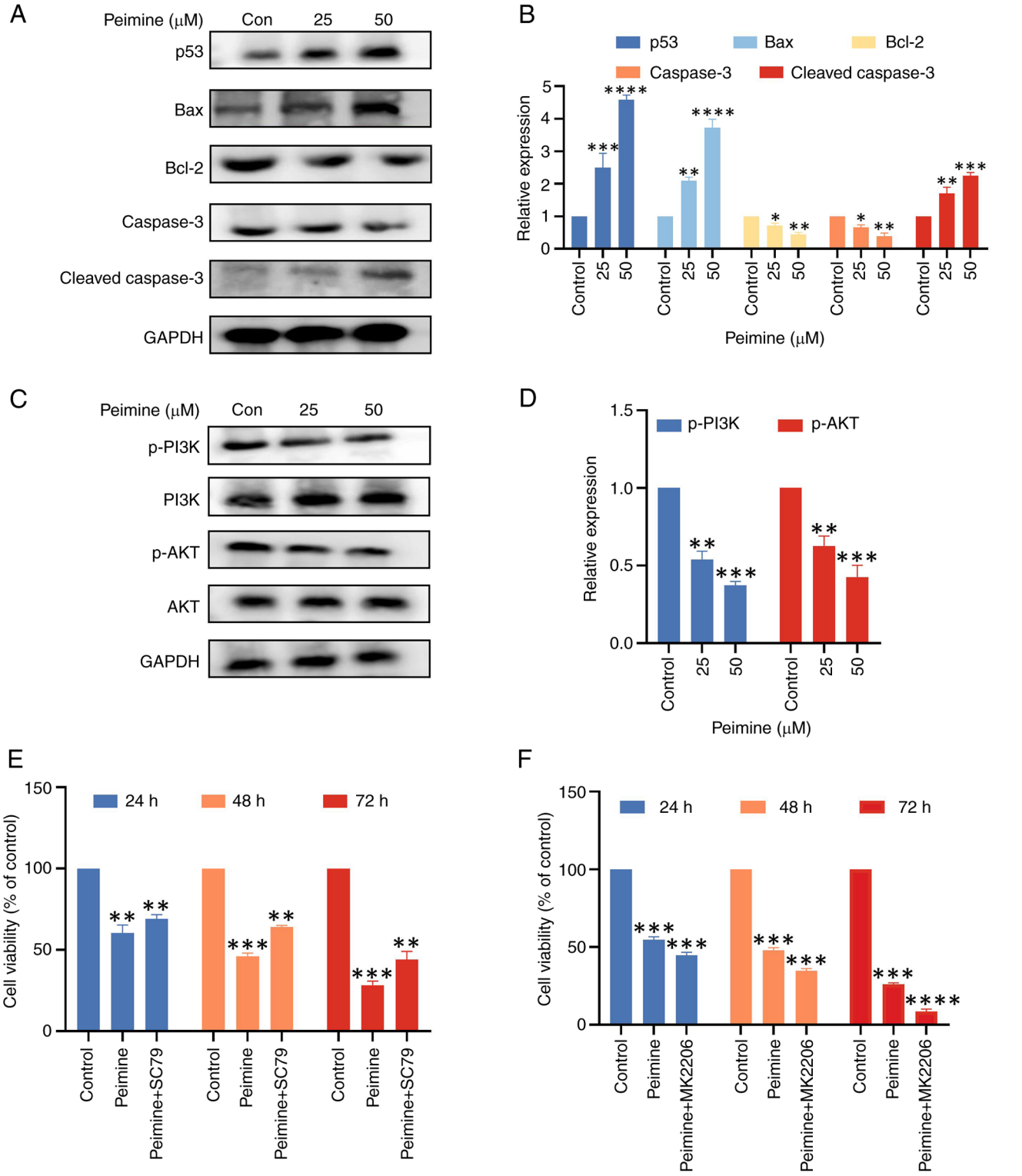

Figure 5. Peimine induces apoptosis in GBM cells through regulation of the PI3K/AKT signaling pathway. (A) Western blot analysis of p53, Bax, Bcl-2, Caspase 3 and Cleaved-Caspase 3 expression in peimine-treated U87 cells. (B) Semi-quantifcation of (A). (C) Western blot analysis of PI3K, p-PI3K, AKT and p-AKT protein levels in peimine-treated U87 cells. (D) Semi-quantification of (C). Cells were pretreated with 0 and 25 μM peimine (E) with or without SC79 pretreatment for 1 h or (F) with or without MK2206 pretreatment for 24 h, before viability was evaluated using an MTT assay. Data were analyzed using a one-way ANOVA followed by a Tukey's post-hoc test. *P<0.05, **P<0.01, ***P<0.001 and ****P<0.0001 vs. control. p-, phosphorylated.

enhance the pharmacological effects of chemotherapy, to improve efficacy and concurrently reduce the side effects (25-28).

The process of apoptosis, a type of programmed cell death (29,30), causes major alterations in the appearance and activity of cells prior to their death (31,32). Apoptotic protein regulation and the activation of complex signaling pathways control this coordinated process (33,34). Peimine was shown in the present study to induce apoptosis via activation of the mitochondrial pathway, whilst also reducing the migration, invasion

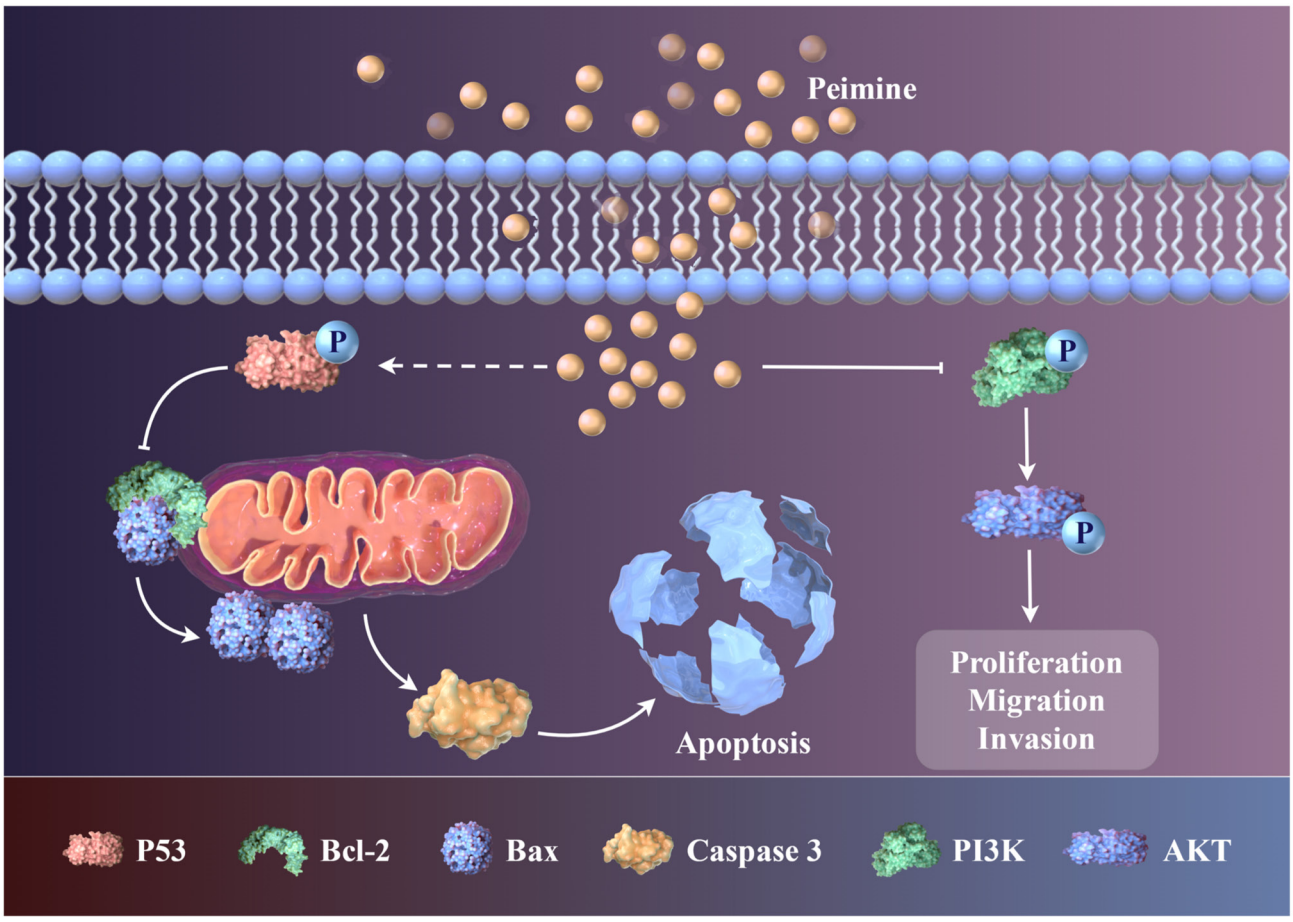

Figure 6. Diagram illustrating how peimine may induce apoptosis in GBM cells through the PI3K/AKT signaling pathway. (Composed using Figdraw). GBM, glioblastoma.

and proliferation of GBM cells. Peimine specifically decreased the mitochondrial membrane potential, promoting Bax, a key step for the irreversible initiation of the caspase cascade. The PI3K/AKT signaling pathway is crucial to the onset and progression of GBM (35,36). Activation of this pathway has been previously associated with the development of GBM by promoting tumor cell proliferation and metastasis, preventing apoptosis and facilitating cell cycle progression (37). In addition, the PI3K/AKT signaling pathway serves as a target of several antitumor drugs, such as peimine, where it is intricately involved in both treatment and resistance mechanisms (38,39). MK2206 is a selective allosteric inhibitor of the AKT signaling pathway. MK2206 specifically targets and inhibits AKT activity by binding to its allosteric site, leading to a decrease in its phosphorylation and subsequent downstream signaling. This inhibition can potentially induce apoptosis in cancer cells and enhance the efficacy of other therapeutic agents, making MK2206 a candidate for targeted cancer therapy, particularly in tumors where the PI3K/AKT pathway is aberrantly activated. In this study, the combination of peimine and AKT inhibitor MK2206 further inhibited the proliferation of U87 cells. Clinical trials and research studies are ongoing to evaluate its effectiveness and safety in breast, gastric and prostate cancer among others, and in combination with other treatments (40-43).

The effects of peimine on GBM were investigated in the present study using multiple experimental approaches, including MTT assays, Transwell assays, measurement of ROS levels and western blot analysis. These methods collectively provided insights into the inhibitory mechanisms of peimine against GBM. Notably, the results suggested that peimine regulated the PI3K/AKT signaling pathway by inducin apoptosis to exert its effects (Fig. 6). Peimine was shown to induce apoptosis in GBM cells, prompting further exploration of its mechanism and potential therapeutic significance in GBM treatment. Although peimine shows promise as an anticancer agent, additional animal experiments,for instance pharmacokinetics and clinical trials, are warranted to fully elucidate and confirm its therapeutic potential. Future research should delve deeper into other signaling pathways involved, such as angiogenesis pathways, and the potential crosstalk between them, and conduct *in vivo* experiments to determine the value of peimine as a targeted small-molecule drug for GBM treatment to determine its precise mechanism of action.

In conclusion, the results of the present study showed that peimine, a novel small-molecule, was a potential therapeutic option for the management of GBM. Peimine inhibited GBM cell proliferation, migration and invasion *in vitro* in a dose-dependent manner and prevented tumor growth without significant drug toxicity *in vivo*. It is important to note that the present study focused on peimine treatment in mouse models of GBM, but did not assess its expression in human tissues, which is a significant limitation. Overall, the results

of the present study showed peimine may hold promise as a novel small-molecule therapeutic agent for the management of GBM.

Acknowledgements

Not applicable.

Funding

The present study was funded by The Science and Technology Research Project of the Hubei Education Department (grant no. B2019161) and the National Natural Science Foundation of China (grant no. 31900853).

Availability of data and materials

The data generated in the present study may be requested from the corresponding author.

Authors' contributions

JL and JY conceived and designed the study, performed the experiments, gathered and evaluated the data, and wrote and edited the manuscript. SC, FL ZihW, ZiyW, ZiqW and CS performed the experiments and collected and analyzed the data. LL assisted with study conception and design, and contributed to the revision of the manuscript. All authors have read and approved the final manuscript. All authors confirm the authenticity of the raw data.

Ethics approval and consent to participate

Hubei University of Science and Technology Animal Ethics Committee approved the animal experiments (approval no. 2022-11-027) and all procedures adhered to national and international standards for the care and use of animals in research.

Patient consent for publication

Not applicable.

Competing interests

The authors declare that they have no competing interests.

References

1. Tamimi AF and Juweid M: Epidemiology and outcome of glioblastoma. In: Glioblastoma. De Vleeschouwer S (ed). Codon Publications, Brisbane, AU, 2017.
2. Batash R, Asna N, Schaffer P, Francis N and Schaffer M: Glioblastoma multiforme, diagnosis and treatment; recent literature review. Curr Med Chem 24: 3002-3009, 2017.
3. Omuro A and DeAngelis LM: Glioblastoma and other malignant gliomas: A clinical review. JAMA 310: 1842-1850, 2013.
4. Siegel RL, Miller KD, Wagle NS and Jemal A: Cancer statistics, 2023. CA Cancer J Clin 73: 17-48, 2023.
5. Dréan A, Goldwirt L, Verreault M, Canney M, Schmitt C, Guehennec J, Delattre JY, Carpentier A and Idbaih A: Blood-brain barrier, cytotoxic chemotherapies and glioblastoma. Expert Rev Neurother 16: 1285-1300, 2016.
6. Schaff LR and Mellinghoff IK: Glioblastoma and other primary brain malignancies in adults: A review. JAMA 329: 574-587, 2023.
7. Fang XH, Zou MY, Chen FQ, Ni H, Nie SP and Yin JY: An overview on interactions between natural product-derived β-glucan and small-molecule compounds. Carbohydr Polym 261: 117850, 2021.
8. McKinnon C, Nandhabalan M, Murray SA and Plaha P: Glioblastoma: Clinical presentation, diagnosis, and management. BMJ 374: n1560, 2021.
9. An YL, Wei WL and Guo DA: Application of analytical technologies in the discrimination and authentication of herbs from Fritillaria: A review. Crit Rev Anal Chem 54: 1775-1796, 2024.
10. Yi PF, Wu YC, Dong HB, Guo Y, Wei Q, Zhang C, Song Z, Qin QQ, Lv S, Wu SC and Fu BD: Peimine impairs pro-inflammatory cytokine secretion through the inhibition of the activation of NF-κB and MAPK in LPS-induced RAW264.7 macrophages. Immunopharmacol Immunotoxicol 35: 567-572, 2013.
11. Xu J, Zhao W, Pan L, Zhang A, Chen Q, Xu K, Lu H and Chen Y: Peimine, a main active ingredient of Fritillaria, exhibits anti-inflammatory and pain suppression properties at the cellular level. Fitoterapia 111: 1-6, 2016.
12. Zhang L, Cui M and Chen S: Identification of the molecular mechanisms of peimine in the treatment of cough using computational target fishing. Molecules 25: 1105, 2020.
13. Zhang T, Liu GY, Cao JL, Li YN, Xue H, Wu HT and Jin CH: Peimine-induced apoptosis and inhibition of migration by regulating reactive oxygen species-mediated MAPK/STAT3/NF-κB and Wnt/β-catenin signaling pathways in gastric cancer MKN-45 cells. Drug Dev Res 83: 1683-1696, 2022.
14. Sun J, Li J, Kong X and Guo Q: Peimine inhibits MCF-7 breast cancer cell growth by modulating inflammasome activation: Critical roles of MAPK and NF-κB signaling. Anticancer Agents Med Chem 23: 317-327, 2023.
15. Tan H, Zhang G, Yang X, Jing T, Shen D and Wang X: Peimine inhibits the growth and motility of prostate cancer cells and induces apoptosis by disruption of intracellular calcium homeostasis through Ca^{2+}/CaMKII/JNK pathway. J Cell Biochem 121: 81-92, 2020.
16. Chen J, Yu Y, Li H, Hu Q, Chen X, He Y, Xue C, Ren F, Ren Z, Li J, *et al*: Long non-coding RNA PVT1 promotes tumor progression by regulating the miR-143/HK2 axis in gallbladder cancer. Mol Cancer 18: 33, 2019.
17. Chen K, Lv ZT, Zhou CH, Liang S, Huang W, Wang ZG, Zhu WT, Wang YT, Jing XZ, Lin H, *et al*: Peimine suppresses interleukin-1β-induced inflammation via MAPK downregulation in chondrocytes. Int J Mol Med 43: 2241-2251, 2019.
18. Tanaka S, Louis DN, Curry WT, Batchelor TT and Dietrich J: Diagnostic and therapeutic avenues for glioblastoma: No longer a dead end? Nat Rev Clin Oncol 10: 14-26, 2013.
19. Le Rhun E, Preusser M, Roth P, Reardon DA, van den Bent M, Wen P, Reifenberger G and Weller M: Molecular targeted therapy of glioblastoma. Cancer Treat Rev 80: 101896, 2019.
20. Zhao W, Zheng XD, Tang PY, Li HM, Liu X, Zhong JJ and Tang YJ: Advances of antitumor drug discovery in traditional Chinese medicine and natural active products by using multi-active components combination. Med Res Rev 43: 1778-1808, 2023.
21. Sevastre AS, Costachi A, Tataranu LG, Brandusa C, Artene SA, Stovicek O, Alexandru O, Danoiu S, Sfredel V and Dricu A: Glioblastoma pharmacotherapy: A multifaceted perspective of conventional and emerging treatments (review). Exp Ther Med 22: 1408, 2021.
22. Wang W, Yuan X, Mu J, Zou Y, Xu L, Chen J, Zhu X, Li B, Zeng Z, Wu X, *et al*: Quercetin induces $MGMT^+$ glioblastoma cells apoptosis via dual inhibition of Wnt3a/β-catenin and Akt/NF-κB signaling pathways. Phytomedicine 118: 154933, 2023.
23. Shen J, Zhang T, Cheng Z, Zhu N, Wang H, Lin L, Wang Z, Yi H and Hu M: Lycorine inhibits glioblastoma multiforme growth through EGFR suppression. J Exp Clin Cancer Res 37: 157, 2018.
24. Luo H, Vong CT, Chen H, Gao Y, Lyu P, Qiu L, Zhao M, Liu Q, Cheng Z, Zou J, *et al*: Naturally occurring anti-cancer compounds: Shining from Chinese herbal medicine. Chin Med 14: 48, 2019.
25. Zhao L, Zhang H, Li N, Chen J, Xu H, Wang Y and Liang Q: Network pharmacology, a promising approach to reveal the pharmacology mechanism of Chinese medicine formula. J Ethnopharmacol 309: 116306, 2023.
26. Hussain A, Brahmbhatt K, Priyani A, Ahmed M, Rizvi TA and Sharma C: Eugenol enhances the chemotherapeutic potential of gemcitabine and induces anticarcinogenic and anti-inflammatory activity in human cervical cancer cells. Cancer Biother Radiopharm 26: 519-527, 2011.
27. Liu Y, Yang S, Wang K, Lu J, Bao X, Wang R, Qiu Y, Wang T and Yu H: Cellular senescence and cancer: Focusing on traditional Chinese medicine and natural products. Cell Prolif 53: e12894, 2020.

28. Wang X, Li J, Chen R, Li T and Chen M: Active ingredients from Chinese medicine for combination cancer therapy. Int J Biol Sci 19: 3499-3525, 2023.
29. Zhang P, Jiang Y, Ye X, Zhang C and Tang Y: PDK1 inhibition reduces autophagy and cell senescence through the PI3K/AKT signalling pathway in a cigarette smoke mouse emphysema model. Exp Ther Med 25: 223, 2023.
30. Wong RS: Apoptosis in cancer: From pathogenesis to treatment. J Exp Clin Cancer Res 30: 87, 2011.
31. Wu Y, Chang J, Ge J, Xu K, Zhou Q, Zhang X, Zhu N and Hu M: Isobavachalcone's alleviation of pyroptosis contributes to enhanced apoptosis in glioblastoma: Possible involvement of NLRP3. Mol Neurobiol 59: 6934-6955, 2022.
32. Bertheloot D, Latz E and Franklin BS: Necroptosis, pyroptosis and apoptosis: An intricate game of cell death. Cell Mol Immunol 18: 1106-1121, 2021.
33. Ketelut-Carneiro N and Fitzgerald KA: Apoptosis, pyroptosis, and necroptosis-oh my! The many ways a cell can die. J Mol Biol 434: 167378, 2022.
34. Attwaters M: Persisting through apoptosis. Nat Rev Mol Cell Biol 23: 697, 2022.
35. Newton K, Strasser A, Kayagaki N and Dixit VM: Cell death. Cell 187: 235-256, 2024.
36. Zhang L, Liu Z, Dong Y and Kong L: E2F2 drives glioma progression via PI3K/AKT in a PFKFB4-dependent manner. Life Sci 276: 119412, 2021.
37. Chautard E, Ouédraogo ZG, Biau J and Verrelle P: Role of Akt in human malignant glioma: From oncogenesis to tumor aggressiveness. J Neurooncol 117: 205-215, 2014.
38. Zhang X, Li Z, Wei C, Luo L, Li S, Zhou J, Liang H, Li Y and Han L: PLK4 initiates crosstalk between cell cycle, cell proliferation and macrophages infiltration in gliomas. Front Oncol 12: 1055371, 2022.
39. Liu F, Chen G, Zhou LN, Wang Y, Zhang ZQ, Qin X and Cao C: YME1L overexpression exerts pro-tumorigenic activity in glioma by promoting Gαi1 expression and Akt activation. Protein Cell 14: 223-229, 2023.
40. Ren J, Zheng S, Zhang L, Liu J, Cao H, Wu S, Xu Y and Sun J: MAPK4 predicts poor prognosis and facilitates the proliferation and migration of glioma through the AKT/mTOR pathway. Cancer Med 12: 11624-11640, 2023.
41. Tang YQ, Li ZW, Feng YF, Yang HQ, Hou CL, Geng C, Yang PR, Zhao HM and Wang J: MK2206 attenuates atherosclerosis by inhibiting lipid accumulation, cell migration, proliferation, and inflammation. Acta Pharmacol Sin 43: 897-907, 2022.
42. Xiang RF, Wang Y, Zhang N, Xu WB, Cao Y, Tong J, Li JM, Wu YL and Yan H: MK2206 enhances the cytocidal effects of bufalin in multiple myeloma by inhibiting the AKT/mTOR pathway. Cell Death Dis 8: e2776, 2017.
43. Cui X, Zhao J, Li G, Yang C, Yang S, Zhan Q, Zhou J, Wang Y, Xiao M, Hong B, *et al*: Blockage of EGFR/AKT and mevalonate pathways synergize the antitumor effect of temozolomide by reprogramming energy metabolism in glioblastoma. Cancer Commun (Lond) 43: 1326-1353, 2023.